Abdominal Imaging

© Springer Science+Business Media, LLC 2008
Published online: 7 September 2008

Abdom Imaging (2009) 34:566–581
DOI: 10.1007/s00261-008-9454-y

Radiologic findings following Y90 radioembolization for primary liver malignancies

Saad M. Ibrahim,[1] Paul Nikolaidis,[2] Frank H. Miller,[2] Robert J. Lewandowski,[1] Robert K. Ryu,[1] Kent T. Sato,[1] Sean Senthilnathan,[1] Ahsun Riaz,[1] Laura Kulik,[3] Mary F. Mulcahy,[4] Reed A. Omary,[1] Riad Salem[1,4]

[1]Section of Interventional Radiology, Department of Radiology, Northwestern Memorial Hospital, Robert H. Lurie Comprehensive Cancer Center, Chicago, IL, USA
[2]Section of Body Imaging, Department of Radiology, Northwestern Memorial Hospital, Chicago, IL, USA
[3]Division of Hepatology, Department of Medicine, Robert H. Lurie Comprehensive Cancer Center, Northwestern University, Chicago, IL, USA
[4]Division of Hematology and Oncology, Department of Medicine, Robert H. Lurie Comprehensive Cancer Center, Northwestern University, Chicago, IL, USA

Abstract

A therapy gaining rapid clinical adoption involves radioembolization with the use of Yttrium-90 (90Y) microspheres. The 20–60 μm-sized microspheres are injected trans-arterially and flow to hepatic tumors given their preferential blood supply from the hepatic artery. Once they lodge in the arterioles, they impart a very intense local radiotherapeutic effect. Given the combined radiation and embolic effect, the imaging findings imparted by this mode of action differ significantly from other treatments. This work represents a comprehensive review of the imaging findings following radioembolization in patients with primary liver tumors. The report discusses imaging response, benign secondary effects, and complications. This should help educate the radiologist on imaging findings that should be expected following radioembolization and therefore aid in the proper image interpretation.

Key words: Radioembolization—Yttrium 90—TheraSphere—SIR-Spheres—Selective—Internal radiation

The two most commonly occurring primary liver malignancies in the world are hepatocellular carcinoma (HCC) and intrahepatic cholangiocarcinoma (ICC). Although both malignancies arise in the liver, the two cancers have very different cellular origins. HCC is a primary malignancy of the hepatocytes whereas ICC arises from biliary ductal tissue.

HCC is the leading cause of primary liver malignancy throughout the world. Although rare in the western hemisphere, HCC is the sixth most common cancer in the world and the third leading cause of cancer-related death [1]. Various factors have been implicated in the malignant transformation of benign tissue; however, the underlying mechanism currently remains unknown [2, 3]. The incidence of HCC is geographically variable with the most commonly identified global risk factor being the hepatitis B carrier state [3]. Other inciting factors include chronic hepatitis C infection, cirrhosis, aflatoxin exposure, alcohol abuse, diabetes mellitus, and hereditary hemochromatosis [4].

ICC is the second most common primary liver malignancy. It accounts for nearly 10–20% of all primary liver tumors. As with HCC, ICC exhibits wide variations in geographic distribution. Although several risk factors have been identified, the etiology and pathogenesis remain poorly understood. Primary sclerosing cholangitis in patients with ulcerative colitis, choledochal cysts or Caroli's disease, hepatolithiasis, exposure to thorotrast agents, and liver fluke infections have all been implicated in cancer induction. Although chronic inflammation and cirrhosis appear to be common denominators associated with the development of both malignancies, their pathogenesis and molecular basis remains elusive.

Correspondence to: Riad Salem; *email:* r-salem@northwestern.edu

The majority of patients diagnosed with these uniformly fatal malignancies present late in the course of their disease and hence are precluded from potentially curative surgical interventions. Depending on patient and tumor characteristics, treatment options include transarterial chemoembolization (TACE), transarterial embolization (TAE), ablative therapies, and supportive care.

In recent years, radioembolization with Y90 microspheres for the treatment of liver malignancies has surfaced with promising outcomes. Transarterial Y90 therapy is unique in that the primary mode of tumor killing is by internal radiation and not induced ischemia. The radiotherapeutic effect is imparted by the infused radioactive microparticles that traverse hepatic vasculature and selectively implant in tumor arteriolar beds. Therein, high energy and low penetrating radiation doses destroy tumor tissue leaving most normal liver parenchyma unharmed. As a result of their distinctive radioactive properties, the imaging findings following therapy do not entirely conform to the radiologic findings that measure therapeutic effectiveness for most traditional therapies. It is therefore necessary to understand the post-treatment imaging features in order to accurately and appropriately interpret the therapeutic effectiveness of Y90 radioembolization.

Device considerations

Transcatheter Yttrium-90 radiotherapy, also known as radioembolization, is a minimally invasive liver directed therapy that selectively delivers internal β-radiation via the arterial vessels that feed tumors. ''Radio'' refers to the radiation that is imparted to tissue; ''embolization'' refers to the microembolic effect [5].

^{90}Y is a pure β-emitter with a physical half-life of 64.2 h, after which it decays into stable zirconium. The average energy of β-emission is 0.9367 MeV, with a mean tissue penetration of 2.5 mm and a maximum penetration of 10 mm. One gigabecquerel (27 mCi) of ^{90}Y per kilogram of tissue provides a dose of 50 Gy.

Two commercially available yttrium-90 microsphere devices are currently available. TheraSphere® (MDS Nordion, Ottawa, Ontario, Canada) is made of glass and SIR-Spheres® (Sirtex Medical, Lane Cove, Australia) are made of resin. These two devices differ in a number of important aspects [6].

^{90}Y glass microspheres

TheraSpheres® are composed of non-biodegradable glass microspheres ranging from 20 to 30 μm in diameter, in which ^{90}Y is an integral constituent of the glass. The microspheres are supplied in 0.5 mL of sterile, pyrogen-free water contained in a 0.3-mL V-bottom vial secured within a 12-mm clear acrylic shield. A 3-GBq vial contains 1.2 million spheres. The specific activity is 2500 Bq at the time of calibration.

^{90}Y resin microspheres

SIR-Spheres® consist of biodegradable resin-based microspheres containing ^{90}Y. The average diameter of a sphere is approximately 35 μm. Upon in vivo administration the spheres are permanently implanted within arterioles. A 3-GBq vial of ^{90}Y contains 40–80 million spheres. The activity per microsphere is 50 Bq at the time of calibration.

The typical method for calculating the required activity with each device, as well as the technical details, have been previously published and will not be discussed further [6–12].

Treatment

Y90 radioembolization targets liver malignancies through the arterial conduits that perfuse them. As a result, angiographic studies are a prerequisite element of this therapy. The angiographic evaluation are conducted to assess visceral anatomy, identify anatomic variants, isolate the hepatic circulation, and determine tumor location for appropriate catheter placement [13].

Angiography is carried out in the following order: (1) abdominal aortogram, (2) superior mesenteric arteriogram, and (3) celiac angiogram. The abdominal aortogram is performed to assess the patency of the superior mesenteric and celiac arteries as well as assess for aortic tortuosity. The superior mesenteric arteriogram is performed to assess for variant arterial anatomy and the patency of the portal vein. A celiac angiogram is performed to evaluate the hepatic arterial vessels, identify additional vascular variants, and determine the tumors' blood supply.

To avoid the complications associated with misdirected microspheres, prophylactic embolization of the extrahepatic vessels is a necessary component of this therapy. This prevents the inadvertent deposition of the microspheres into areas other than the neoplastic vasculature. The severe adverse events associated with unplanned administrations have been previously published; only the imaging findings will be discussed in this paper [14–20].

Patient selection

The ideal patient with primary liver malignancy is only selected for radioembolization after undergoing a thorough medical examination. Evaluation includes a complete history and physical assessment of laboratory values including tumor markers, determining the severity of liver disease (Child-Pugh, Okuda, etc.), and assessing baseline performance status. Patients with primary liver malignancy should be staged appropri-

ately prior to treatment (BCLC, CLIP, UNOS, etc.). They should have liver-only or liver-dominant disease. Patients must have adequate liver and renal function and a predicted life expectancy of greater than 3 months in order to be considered. Despite fulfilling the aforementioned criteria, patients should also not demonstrate significant hepatopulmonary shunting at technetium-99 macroaggregated scintigraphy. Patients likely to receive greater than 30 Gy of radiation at treatment or greater than 50 Gy at multiple sessions should theoretically be excluded. Additionally, patients with significant hepatogastrointestinal shunting, not correctable by modern catheter technique, should be excluded.

Oncologic response assessment

Size criteria, as assessed by conventional radiographic modalities (MRI/CT), have traditionally been the standard by which the therapeutic efficacy of a given treatment is assessed [21]. Anatomic measurements are often heavily relied upon to assess treatment response.

Following Y90 radioembolization, the use of strict anatomic criteria alone has been shown to be an imperfect evaluation of therapeutic response [22]. Erroneous radiologic interpretation of findings such as an incomplete response to treatment or apparent tumor progression are often observed in the early follow-up period. In certain instances, benign findings are confused with pathologic findings [23].

Herein we will describe the common imaging features in patients with HCC and ICC following Y90 therapy. Size and necrosis criteria, tumor marker reduction, in addition to other novel functional imaging modalities (diffusion-weighted MRI and PET) to assess post-radioembolization responses will be discussed. Furthermore, we will show by example, unique benign findings that may appear as pathologic. Finally, the potential treatment-related complications associated with this therapy will be discussed.

Tumor reduction

Conventional imaging modalities such as computed tomography (CT) and magnetic resonance imaging (MRI) use the morphologic features of a tumor to establish the extent of disease. The presence and degree of tumor shrinkage, as assessed by strict anatomic criteria, is the standard by which oncologic response and therapeutic effectiveness of a given therapy is measured. Until 2000, World Health Organization (WHO) criteria utilizing bidimensional anatomic measurements were the standard by which tumor reductions were calculated. In 2000, however, newer guidelines were established, known as the Response Evaluation Criteria in Solid Tumors (RECIST), which set a new standard for assessing and reporting tumor response [21]. The new criteria are based on the measurement of the single longest tumor diameter and have since been criticized for their limitations. To fully appreciate the efficacy of Y90 radioembolization, changes in anatomic size must be considered in combination with other useful imaging techniques (necrosis, PET, and DW-MRI—to be discussed) in order to determine the therapeutic benefits. By size criteria alone, the partial response rate reported for radioembolization has been between 20% and 40% [24–26].

Tumor necrosis

Following cytoreductive therapies such as radiofrequency, microwave, thermal or ethanol ablation, strict size criteria alone often fail to demonstrate tumor response and therapeutic effect. Analogously, at early follow-up imaging after embolotherapy with Y90 (or other embolics), liver tumors may shrink (Figs. 1, 2), appear larger (Fig. 3), or not change at all in size (Fig. 4). This creates specific problems, at least when lesions appear larger, for patients treated with the intent to be downstaged and bridged to potentially curative surgical interventions. As a result of this limitation, the European Association for the Study of the Liver (EASL) made specific recommendations to account for non-viable tissue following these therapies [27]. The recommendations from this expert panel were to account for necrosis (cellular death and coagulative processes) by appreciating areas of non-enhancing tissue with contrast-enhanced helical CT. Using this criterion to assess response following Y90 for hepatocellular carcinoma was first reported by Keppke et al (Figs. 3, 4) [22]. The authors showed that the median time to response using size criteria alone was approximately 120 days, whereas it was only 30 days by necrosis criteria. Response rates using necrosis criteria following Y90 therapy have been between 70% and 90% [25, 28].

Diffusion-weighted magnetic resonance imaging (DW-MRI)

The use of DW-MRI for detecting early post-treatment tumor response has been explored in several series [29, 30]. Diffusion-weighted imaging (DWI) allows for tissue characterization without the need for utilization of contrast agents [31]. This technology uses water mobility as an in vivo probe for interrogating tissue microstructure. Studies with both transarterial chemoembolization (TACE) and Y90 radioembolization have shown that DW-MRI may represent a sensitive clinical biomarker in the early follow-up period to assess Y90 therapy response [30, 32] (Fig. 5). This may have important clinical and prognostic implications for pa-

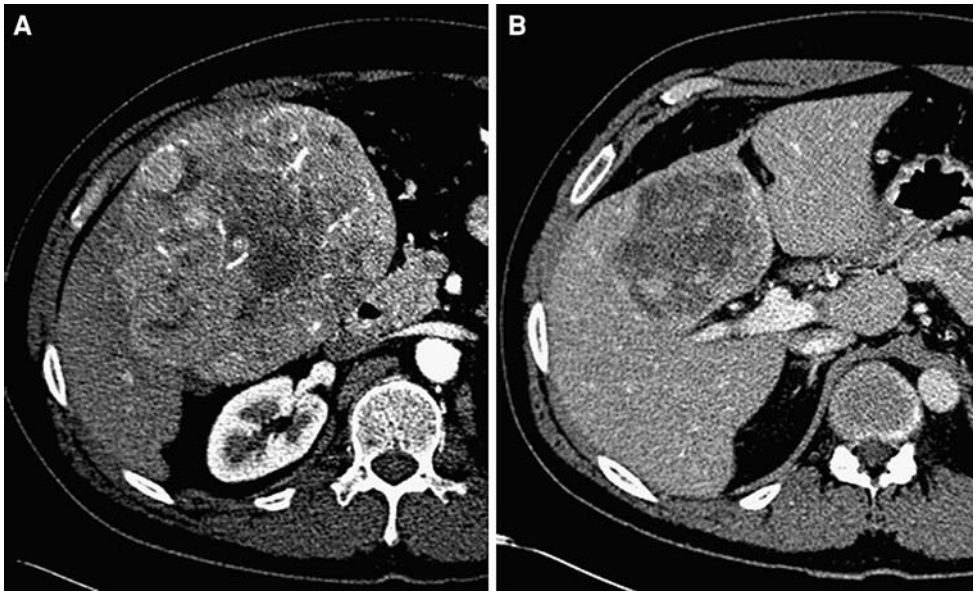

Fig. 1. (**A**) Pre-treatment contrast-enhanced CT demonstrates a large, 17 cm, heterogeneously enhancing exophytic hepatoma. (**B**) Post-treatment contrast-enhanced CT demonstrates significant reduction in tumor size and enhancement. The tumor now measures 7 cm.

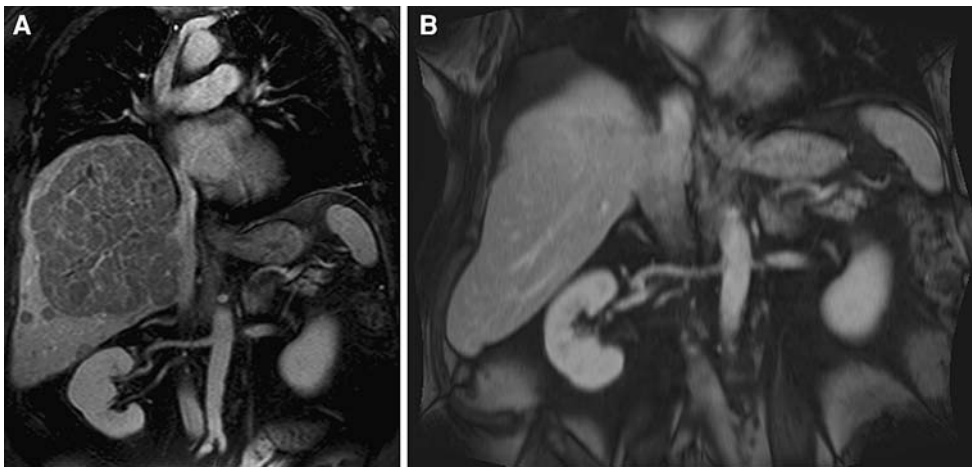

Fig. 2. (**A**) Pre-treatment T1-weighted gadolinium-enhanced MRI in the coronal plane demonstrates a well large right lobe hepatoma with satellite lesions. Tumor burden exceeds 75% of the liver. (**B**) At 22 months after one treatment with Y90 and no adjuvant therapy, T1-weighted gadolinium-enhanced MRI in the coronal plane demonstrates marked size reduction with near complete resolution of the tumor mass.

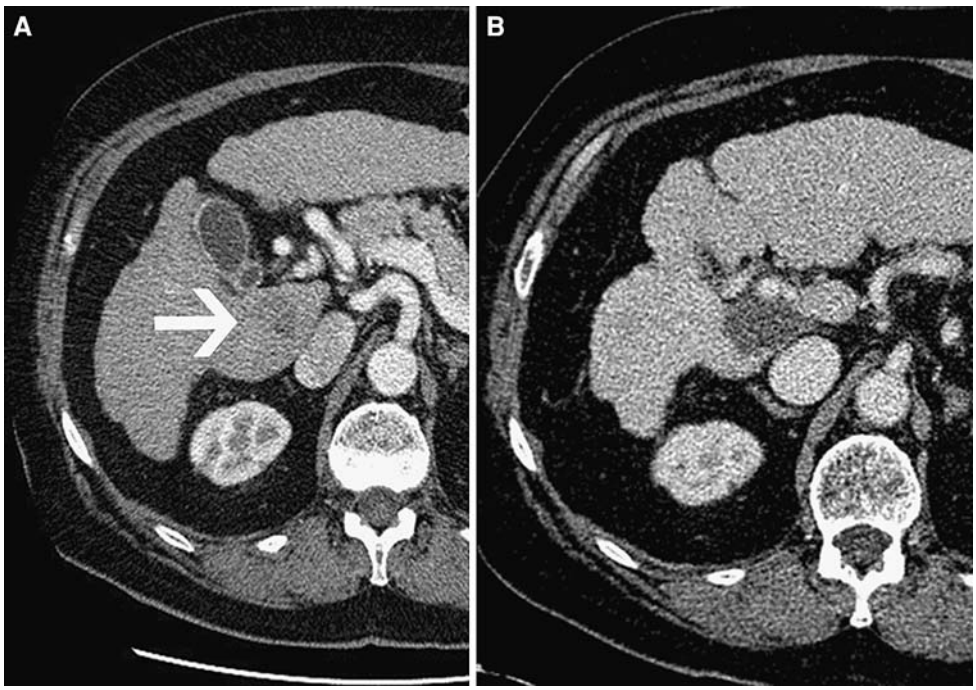

Fig. 3. (**A**) Pre-treatment contrast-enhanced CT demonstrates a cirrhotic liver with a caudate lobe (segment 1) hepatoma (*arrow*). (**B**) At 2-year imaging follow-up, contrast-enhanced CT scan demonstrates not only complete necrosis and avascularity of the radioembolized segment 1 hepatoma, but an increase in the size of the lesion. Using traditional size criteria this lesion would be considered stable disease as opposed to complete response by necrosis criteria.

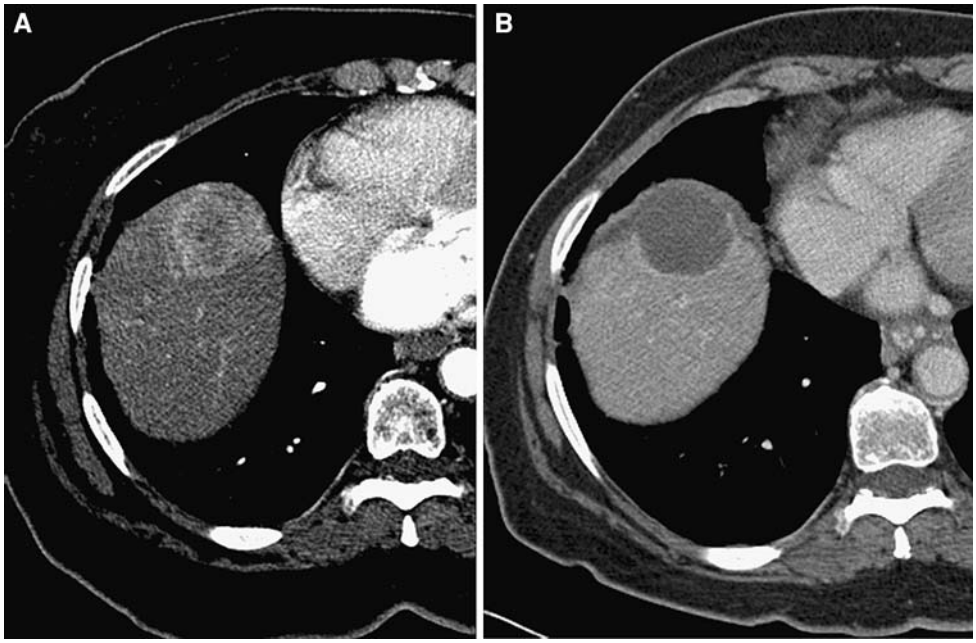

Fig. 4. (**A**) Pre-treatment contrast-enhanced CT demonstrates a focal heterogeneously enhancing hepatic dome hepatoma. (**B**) Post-treatment contrast-enhanced CT demonstrates complete necrosis and lack of change in size of mass. Note the slight peripheral enhancement seen at the border with normal hepatic parenchyma. The peripheral enhancement is not due to tumor.

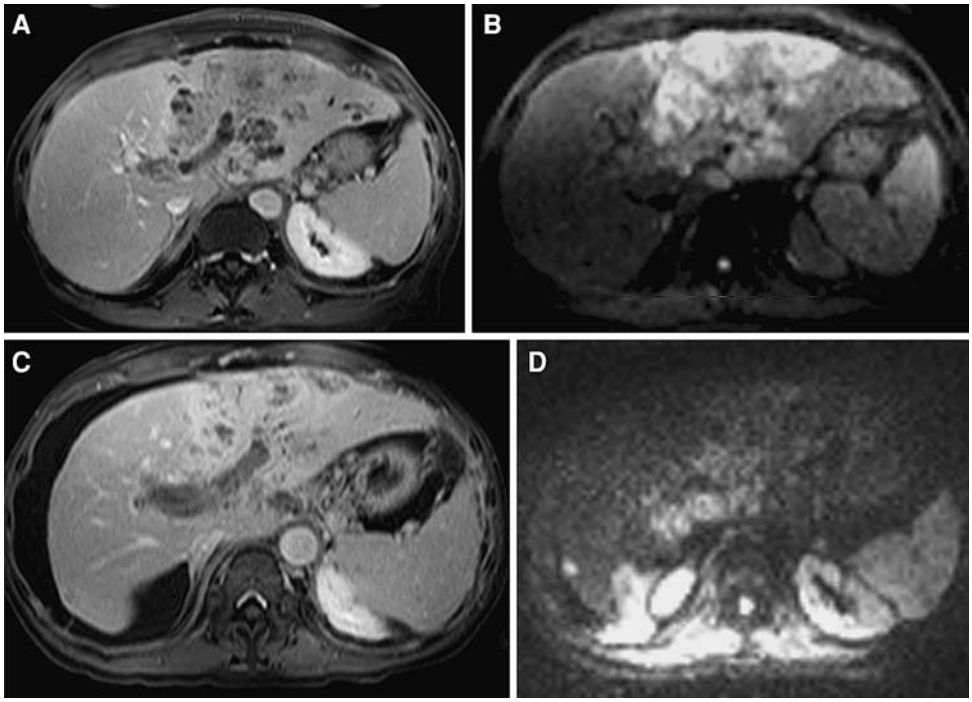

Fig. 5. (**A**) Pre-treatment gadolinium-enhanced MRI shows a large heterogeneous mass in the left lobe of the liver. The margins are difficult to define. (**B**) Pre-treatment DW-MRI differentiates the tumor from the surrounding liver. The tumor has restricted diffusion and the margins are well defined. (**C**) Post-treatment gadolinium-enhanced MRI shows enhancement of the left lobe of the liver. It is difficult to assess response as the tumor is not well defined. (**D**) Post-treatment DW-MRI shows a response with the mass showing less restricted diffusion and appearing significantly smaller. A new lesion is seen in the right lobe of the liver.

tients treated with Y90 radioembolization. Investigators showed the utility of DW-MRI in detecting and predicting tumor response was approximately 42 days following Y90 therapy [30]. Increased tumor tissue water mobility after therapy is presumably related to both reduced cellularity and compromised cell membrane integrity. As a result, water mobility studies may potentially differentiate viable tumor from benign tissue.

^{18}F-fluorodeoxyglucose positron electron tomography (^{18}FDG-PET)

Positron electron tomography (PET) is a metabolic imaging modality that is used for diagnosing, staging, and managing a vast array of tumors. As a result of the increased glucose transport, metabolism, and utilization, malignant cells avidly accumulate FDG [33]. Studies have shown the high sensitivity and specificity of FDG-

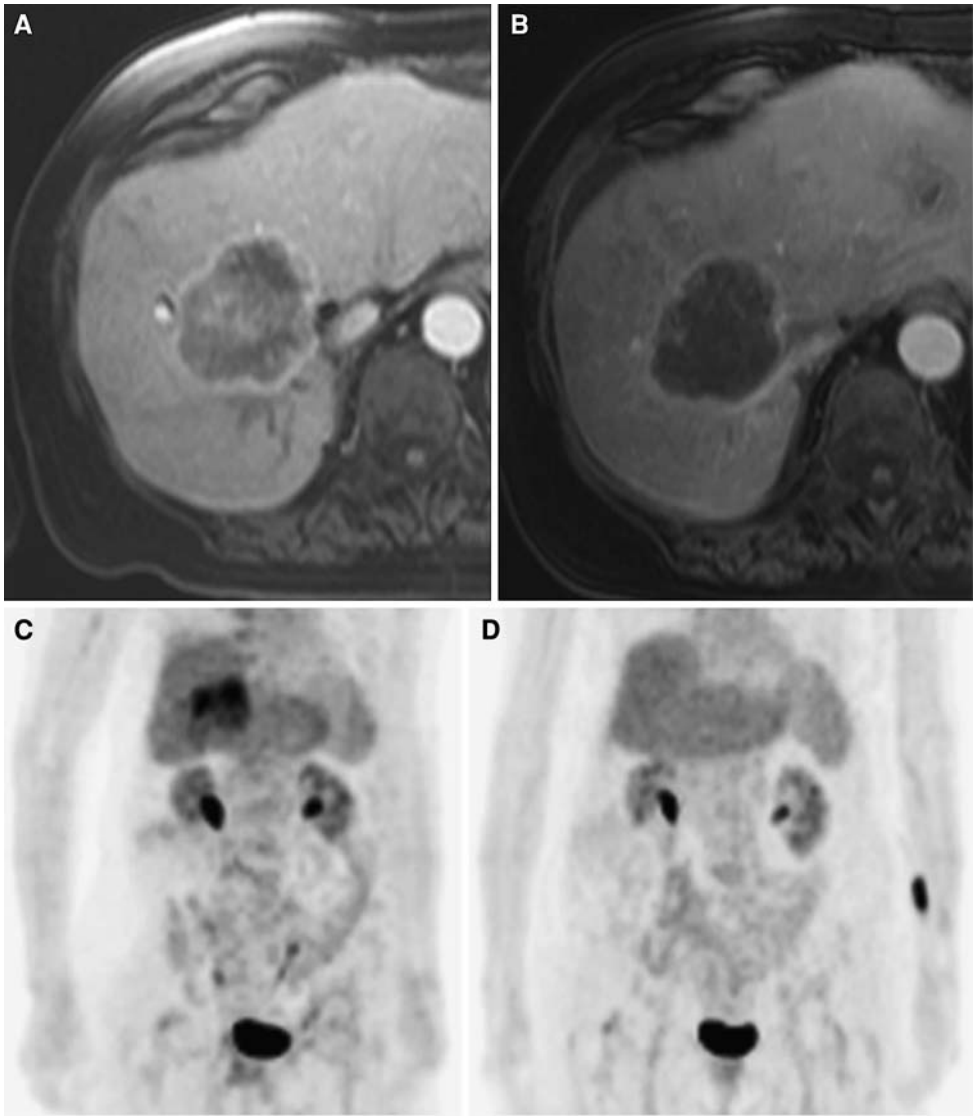

Fig. 6. (**A**) T1-weighted contrast-enhanced MRI demonstrates a ring-enhancing solitary cholangiocarcinoma within hepatic segments 4–8. (**B**) Following treatment, T1-weighted gadolinium-enhanced MRI demonstrates rim enhancement with near complete necrosis. The cholangiocarcinoma did not decrease in size and represents stable disease by size criteria. (**C**) Pre-treatment coronal FDG-PET in the same patient as Fig. 6A/B (cholangiocarcinoma) demonstrates a hypermetabolic FDG avid ICC. (**D**) Post-treatment follow-up PET demonstrates complete resolution with no discernable increased activity in the liver.

PET for detecting tumor recurrence in patients with colorectal cancer liver metastases. Additionally, PET imaging has demonstrated the ability to show post-Y90 responses earlier than traditional anatomic imaging modalities for patients with hepatic metastases [34]. PET is a useful adjunct to conventional imaging modalities in determining overall post-therapeutic response (Fig. 6). Although its utility for assessing response in patients with HCC and ICC remains unclear, selected patients demonstrate favorable PET response following therapy. The overall PET response rate for patients with hepatic metastatic disease has been between 60% and 80% [35, 36]. For HCC or ICC, the PET response rate has not been elucidated.

Tumor marker response

Tumor marker reductions following Y90 radioembolization will often signify favorable response to therapy. This reduction generally translates to better prognosis and overall survival for the responding patient. Tumor marker response following Y90 therapy, however, has not been shown to correlate with anatomic imaging response. There does appear to be some concordance between the extent of tumor necrosis and reduction in AFP levels following therapy. Interestingly, not all patients with HCC have elevated serum AFP levels. Therefore, for patients with elevated baseline pre-treatment serum AFP values, post-treatment reductions may serve as an important biomarker to assess response to therapy (Fig. 7) [27]. Other tumor markers for patients with HCC have been described but have yet to be validated (AFP-L3, DCP, PIVKA II).

The sensitivity and specificity of tumor markers for detecting cholangiocarcinoma are low. A patient may or may not present with elevated levels of the three most commonly tested markers (CA 19-9, CEA, CA 125). Several additional serum tumor markers have been linked to

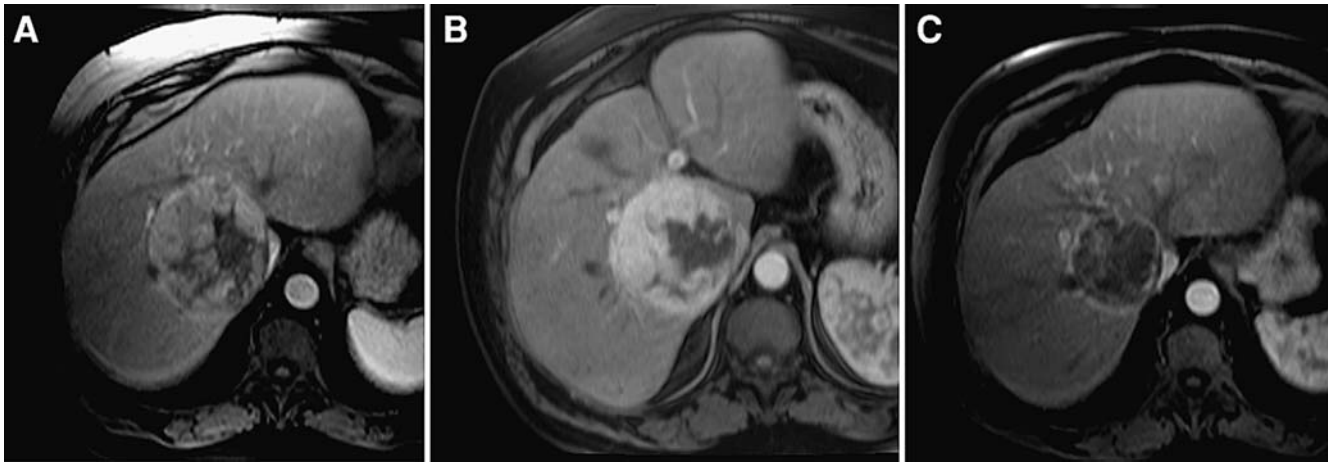

Fig. 7. (**A**) Pre-treatment gadolinium-enhanced T1-weighted MRI demonstrates a heterogeneously enhancing caudate lobe (segment I) hepatoma. Serum AFP value was 2,200 ng/dL. (**B**) At 1 month follow-up imaging, gadolinium-enhanced T1-weighted imaging demonstrates the enhancing caudate hepatoma with no change in tumor size. Tumor is categorized as stable disease by size criteria. Serum AFP values dropped to 125 ng/dl, representing a 94.3% reduction. Rather than retreat, the patient was observed and a 3-month MRI scheduled. (**C**) At 3-month follow-up, without further intervention or repeat treatment, gadolinium-enhanced T1-weighted imaging demonstrates complete necrosis and avascularity of the caudate lobe hepatoma. There is very little tumor shrinkage and thus no change in categorization (stable disease by size criteria). Serum AFP values continued to decline to 3 ng/dL, representing a 99.9% reduction.

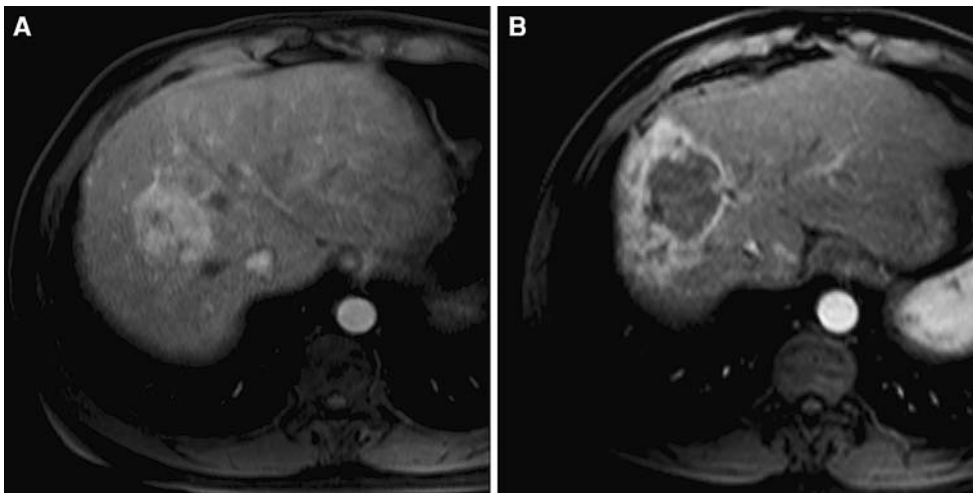

Fig. 8. (**A**) T1-weighted contrast-enhanced MRI shows an arterially enhancing hepatoma in the right hepatic lobe. (**B**) Following Y90, T1-weighted gadolinium-enhanced MRI demonstrates tumor necrosis and surrounding hepatic parenchymal hyperenhancement from radiation occurring in a perivascular distribution.

cholangiocarcinoma including CA-195, DU-PAN 2, and CA-242, but their role at this time is not clear. There is no evidence that serum tumor marker measurements are useful for monitoring disease progression [37].

Benign treatment-related findings

Perivascular edema

Perivascular edema following Y90 therapy has been previously reported in the literature. No pathologic basis for these findings has been identified—in essence these imaging findings are benign and related to the microsphere distribution and intense radiotherapeutic effect exerted by the microspheres—once they become lodged in the peritumoral vascular plexus. Without knowledge of this phenomenon, perivascular edema may be incorrectly ascribed as infiltrative disease (Fig. 8). The findings are only transient and persist for 3–6 months following therapy.

Ring enhancement

Previous studies have shown that peritumoral ring enhancement following therapy is not necessarily indicative of viable tumor. Investigators observed a high correlation between the imaging findings of peripheral ring enhancement and complete pathologic necrosis on the explant specimens from 20 patients that were either bridged or downstaged to resection or transplantation [24, 38].

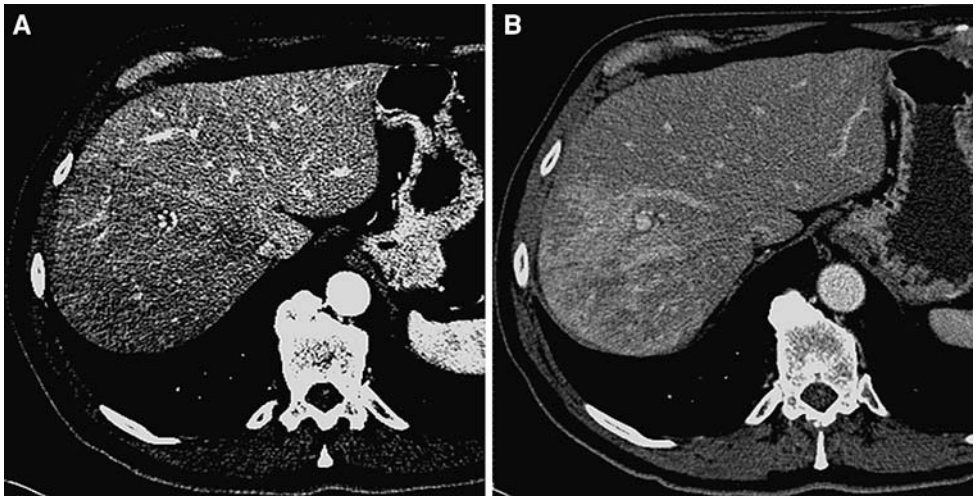

Fig. 9. (**A**) Contrast-enhanced CT in the arterial phase demonstrates diffuse hypoattenuating parenchyma in the right hepatic lobe distribution following Y90. (**B**) In a different patient from (**A**), contrast-enhanced CT scan demonstrates parenchymal hyperenhancement from radiation effect in the right hepatic artery distribution following treatment for a right lobe hepatoma.

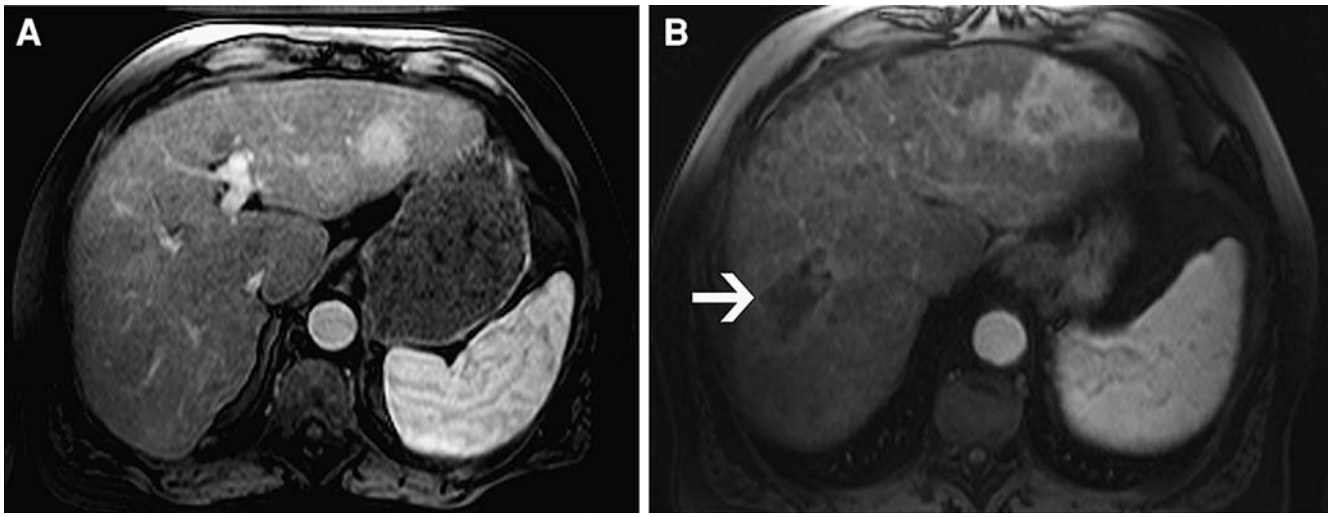

Fig. 10. (**A**) Prior to treatment, T1-weighted contrast-enhanced MRI demonstrates a homogeneously enhancing mass in the left hepatic lobe, consistent with a hepatoma. (**B**) Following segmental infusion of Y90, contrast-enhanced MRI demonstrates rim enhancement and tumor necrosis. Note the parenchymal hyperenhancement due to radiation effect occurring in a vascular (wedge) distribution. *Arrow* demonstrates area of necrosis from a previous right lobe treatment. Patient had serum AFP reductions of 99.2% and was bridged to orthotopic liver transplantation.

Radiation effect

Radiation effect in a treated segment/lobe is a common imaging finding following Y90 radioembolization. The radiation territory as seen on imaging studies exactly delineates the vascular territory corresponding to the treated segments or lobes. This is also a benign finding that may mimic progressive infiltrative tumor (Figs. 9, 10). This usually occurs in the absence of liver decompensation or alterations in liver function tests.

Radiation segmentectomy

"Radiation segmentectomy" refers to the selective delivery of an extremely high radiation dose to a targeted hepatic segment. By limiting the radiation to segmental hepatic anatomy, patients are theoretically able to tolerate these radiation doses without developing the potentially fatal complications of radiation-induced liver disease [39]. This technique is particularly applicable in those patients with poor hepatic reserve; the highly selective delivery of the radiation dose to a specific and focal anatomic location limits radiation injury to non-cancerous hepatic parenchyma (Fig. 11).

This technique requires comprehensive and careful hepatic angiography prior to treatment. Proper hepatic arterial catheter positioning can be aided with the use of CT imaging. Rhee et al. have shown that CT angiography facilitates this segmental targeting of tumors, enabling statistically significant higher radiation doses [40].

Hepatic fibrosis and portal hypertension

Radiation therapy has been shown to cause hepatic injury and induce fibrotic change (Fig. 12). As a result of

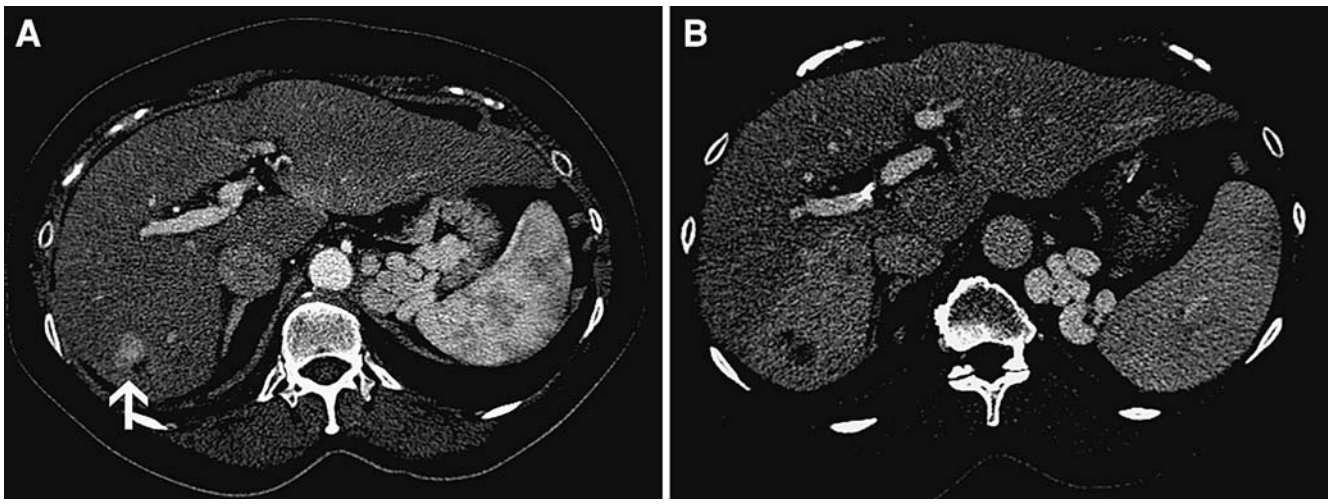

Fig. 11. (**A**) Pre-treatment contrast-enhanced CT demonstrates a solitary segment VII posterior right lobe hepatoma (*arrow*) in a patient with portal hypertension and thrombocytopenia. Patient was a transplant candidate and therefore not ablated due to the risk of tract seeding. (**B**) Post-treatment, contrast-enhanced CT scan demonstrates parenchymal hyperenhancement and radiation effect following a segmental infusion. Note the necrotic tumor in segment VII.

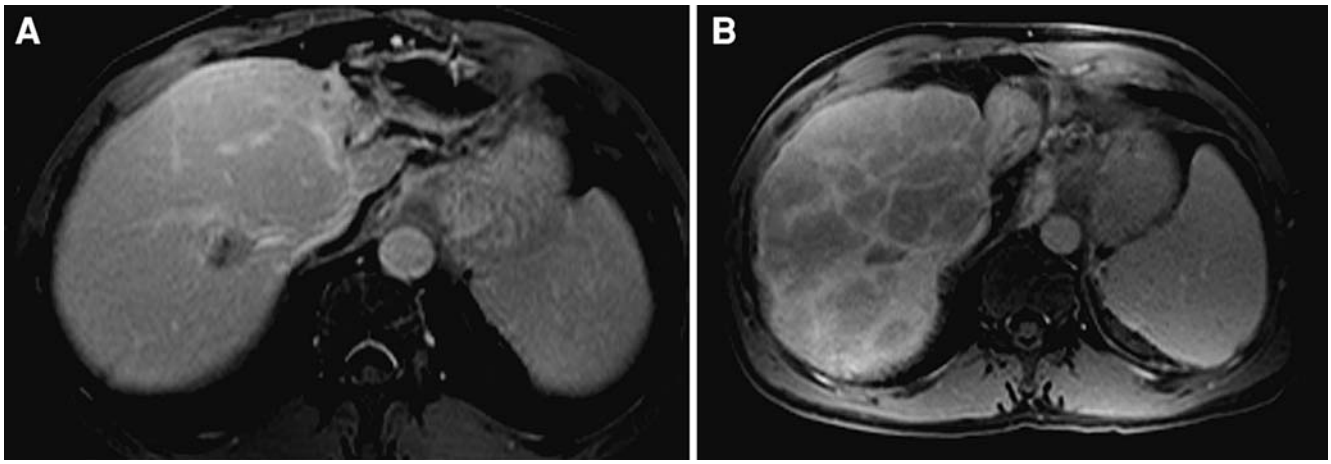

Fig. 12. (**A**) Contrast-enhanced T1-weighted MRI demonstrates a focal mass in the right hepatic lobe prior to Y90 treatment. (**B**) Contrast-enhanced T1-weighted imaging at 2-year follow-up demonstrates heterogeneous enhancement of the hepatic parenchyma with capsular retraction, consistent with hepatic fibrosis in the Y90-treated right hepatic artery distribution.

these changes, regional blood flow through the liver is altered and portal hypertension may ensue. This Y90-induced complication was first described in a study by Jakobs et al. in which 32 patients with metastatic liver disease received treatment to one or both hepatic lobes [41]. The investigators reported a statistically significant volume reduction in the treated lobes following therapy. Statistically significant ipsilateral atrophy with concomitant contralateral hypertrophy was observed in patients following unilobar Y90 treatment (Figs. 13, 14). Patients with bilobar treatment showed evidence of bilateral volume reduction with significantly increased splenic volumes. In the hypertrophied lobe, the authors noted significant increase in the diameter of portal veins perfusing the hypertrophied lobes. Despite the occurrence of fibrosis in these patients, there were no cases of liver failure. A similar clinical finding can occur in patients with both HCC and ICC following Y90 therapy.

Analogously, patients with limited liver reserve may undergo portal vein embolization (PVE) prior to extensive hepatic resection and achieve similar results. Patients are prospectively evaluated and considered for PVE if the future liver remnant following resection (hepatic segmentectomy/lobectomy) is incapable of handling appropriate physiologic demands. The portal vein perfusing the diseased liver is occluded with an embolic agent, resulting in changes in regional blood flow. Blood is shunted away from the diseased liver and in the direction of the non-

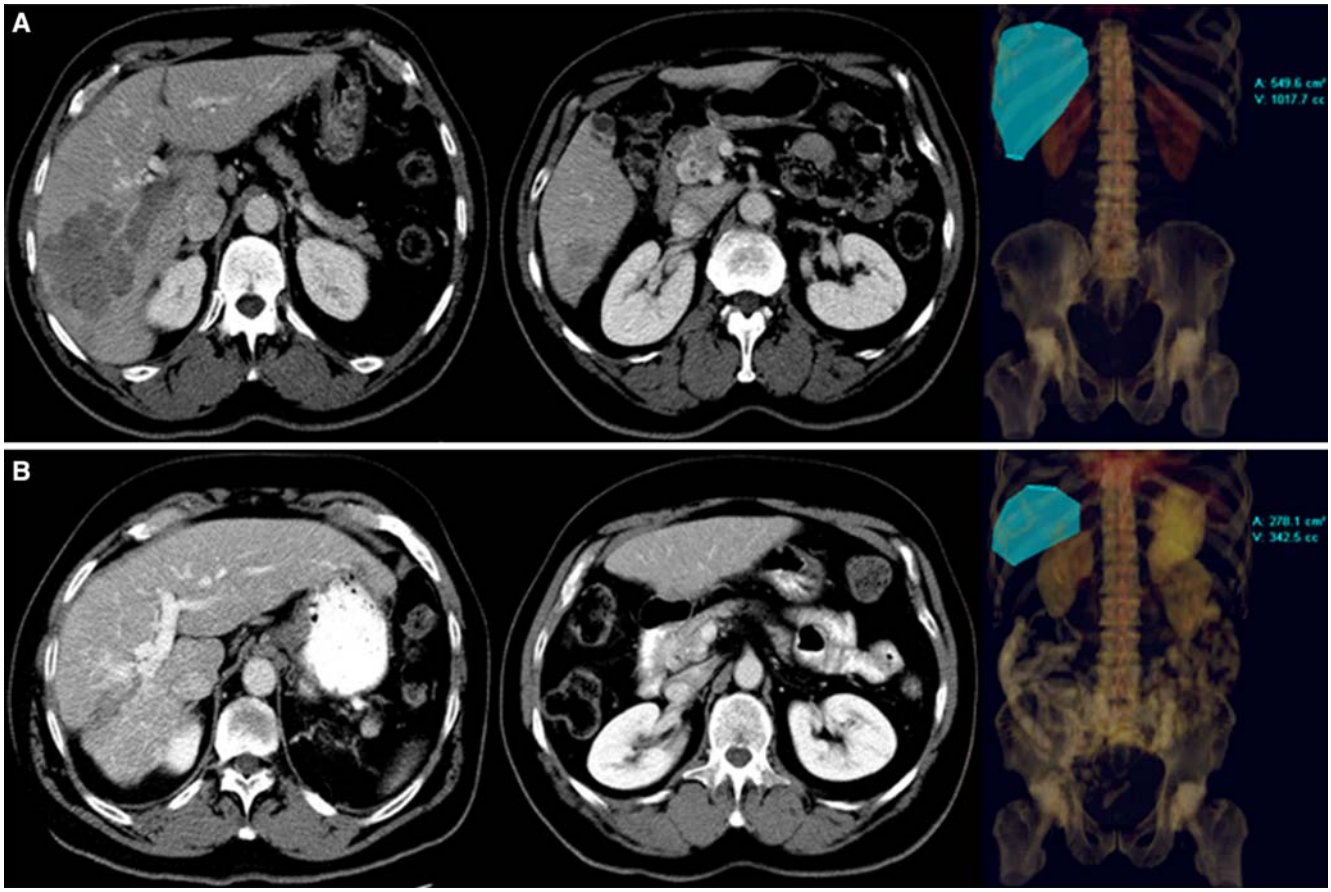

Fig. 13. (**A**) Pre-treatment imaging. (i) Contrast-enhanced CT demonstrates a large lobulated hepatoma with associated right portal vein thrombosis. (ii) In the same patient, pre-treatment contrast-enhanced CT scan demonstrates a small left hepatic lobe in relation to the right hepatic lobe. (iii) Volumetric 3D reconstruction demonstrates a pre-treatment right hepatic lobe volume of 1017.7 cc (right image). (**B**) Post-treatment Imaging. (i) Contrast-enhanced CT scan demonstrates marked tumor size reduction, portal vein retraction, recanalization of the vein, and right lobe capsular retraction. (ii) At a comparable level to Fig. 13b-ii middle image above, post-treatment contrast-enhanced CT scan demonstrates significant left lobe hypertrophy with the non-visualization of the right hepatic lobe. (iii) On post-treatment volumetric 3D reconstruction, the right hepatic lobe volume decreased to 342.5 cc, a 66% reduction (right image).

diseased future remnant. These changes culminate in ipsilateral atrophy of the diseased liver with contralateral hypertrophy of non-diseased hepatic parenchyma (radiation lobectomy).

Benign findings

Bilomas, abscesses, strictures

Biliary complications arising from external beam radiation therapy to the hepatic parenchyma have been well described in the literature [42, 43]. During Y90 infusion, radioactive microspheres may potentially embed within the arterioles of the peribiliary plexus causing similar microscopic injury [44]. Injuries to the biliary tree may manifest as biliary necrosis, bilomas (Fig. 15), abscesses, and/or strictures. These findings occur more often in patients with metastatic liver disease and only rarely in patients with primary liver tumors [45].

In a large single institutional study, Atassi et al. studied the biliary consequences of Y90 radiotherapy in 327 patients [46]. Based on imaging studies and serologic tests, 33 patients (10.1%) had findings indicative of biliary complications. Of the 33 patients, 7 had primary liver tumors (HCC). Biliary necrosis was identified in 6 patients. Three of these patients required percutaneous drainage for bilomas. Two additional patients underwent cholecystectomy for radiation-induced cholecystitis. One patient was treated for a hepatic abscess and 8 patients had biliary strictures visible on follow-up examinations. The instances of biliary strictures were without clinical sequelae and did not necessitate treatment.

Gallbladder wall hyperenhancement

Gallbladder wall hyperenhancement and defects following Y90 radioembolization have been previously pub-

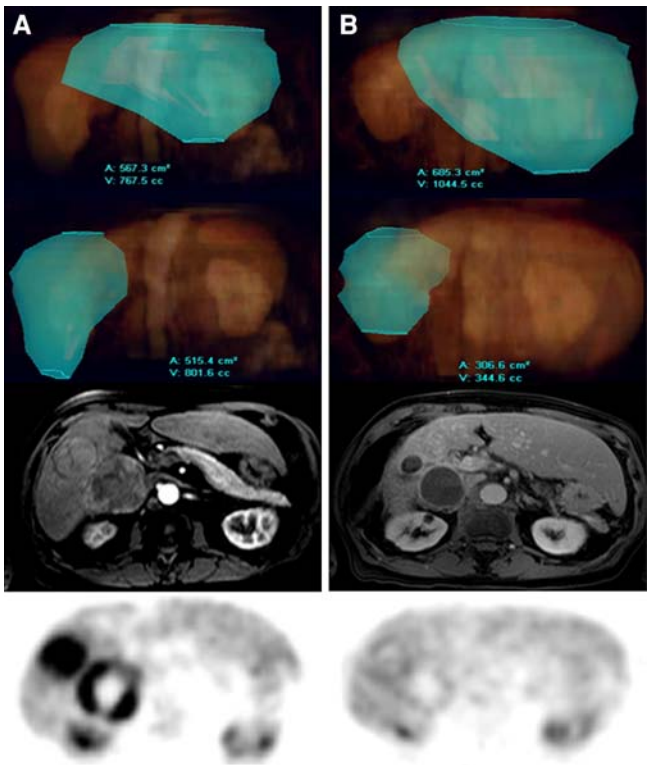

Fig. 14. (**A**) Pre-treatment imaging. Volumetric 3D reconstruction demonstrates a left hepatic lobe and right hepatic lobe volume of 767.5 cc (image i) and 801.6 cc (image ii), respectively. Post-gadolinium T1-weighted MRI demonstrates two large well-circumscribed hepatomas (image iii). Pre-treatment functional axial PET scan demonstrates intense focal uptake of FDG in the HCCs (image iv). (**B**) Following Y90 treatment to the right hepatic lobe, the left hepatic lobe volume has increased 27% to 1044.5 cc (image i) and the right hepatic lobe volume decreased 43% to 346.6 cc (image ii). T1-weighted gadolinium-enhanced MRI demonstrates markedly reduced size of hepatomas with rim enhancement and complete necrosis (image iii). Note the right hepatic lobe retraction and volume reduction compared to the left hepatic lobe hypertrophy. Functional axial PET scan demonstrates marked reduction in the activity and complete resolution (image iv).

lished (Fig. 16) [46]. Atassi et al. reported on 6 patients, from a cohort of 327 patients, which demonstrated gallbladder wall enhancement and focal gallbladder wall disruption on follow-up imaging. Although rarely a complication, radioactive microspheres may embed in the arterioles of the gallbladder mucosa. Entry is generally through the cystic artery; however, perforator arteries and the gastroduodenal artery have also been implicated in non-Y90 type embolic treatments. The most common radiographic findings are increased gallbladder wall enhancement with thickening and mural rents. For the majority of patients, this occurred without clinical sequelae [23].

Treatment-related complications

Radiation cholecystitis

Rarely patients may present with biliary dyskinesia, fever, nausea, and symptomatic right upper quadrant pain following treatment. The first step in the management of such a patient would be to explore conservative therapeutic measures following appropriate radiologic imaging (Fig. 17). If a gallbladder wall perforation is imminent or has already occurred, surgical intervention (ie. cholecystectomy) becomes mandatory for symptomatic patients [23].

Radiation-induced biliary complications

Although biliary complications following Y90 are rarely reported, they do occur albeit usually without clinical consequences. In instances where biliary injury requires treatment, conservative measures usually suffice. In the very rare event a patient is refractory to medical management, endoscopic, percutaneous, or surgical interventions may be required. The biliary complication rates after Y90 treatment are very low. Therefore, it is imperative for the treating physician and radiologist reading the imaging studies are cognizant of these potential complications so that immediate intervention may be initiated ensuring the best overall outcome.

Gastroduodenal ulceration

Non-target radiation administration caused by misdirected radioactive microspheres is a dreaded complication of this transarterial therapy. Reports of gastritis, gastrointestinal ulceration, and other gastrointestinal complications have repeatedly surfaced over the past several years, likely due to the increasing use of this technology (Fig. 18). Variant hepatic arterial anatomy, collateral circulation, changes in flow dynamics, and operator error have been implicated for these complications [47]. Proper techniques and appropriate measures to mitigate these complications have been previously published [44, 48, 49]. In brief, meticulous angiographic technique with an exhaustive interrogation of the hepatic vasculature should be routinely carried out. During evaluation, visceral vasculature should be assessed for the presence of anatomic variants and extrahepatic vessels should be prophylactically embolized with coils. Correct identification and isolation of the hepatic vasculature are essential before microsphere injection. Knowledge of the mesenteric anatomic variants is crucial for the safe and effective delivery of this therapy.

Radiation-induced liver disease (RILD)

External beam radiation therapy has traditionally played a limited role for treating liver tumors due to the radia-

Fig. 15. (**A**) Post-treatment contrast-enhanced CT in the arterial phase demonstrates a fluid collection representing a small biloma. (**B**) In the same patient as Fig. 15A, the coronal view also confirms the presence of the biloma.

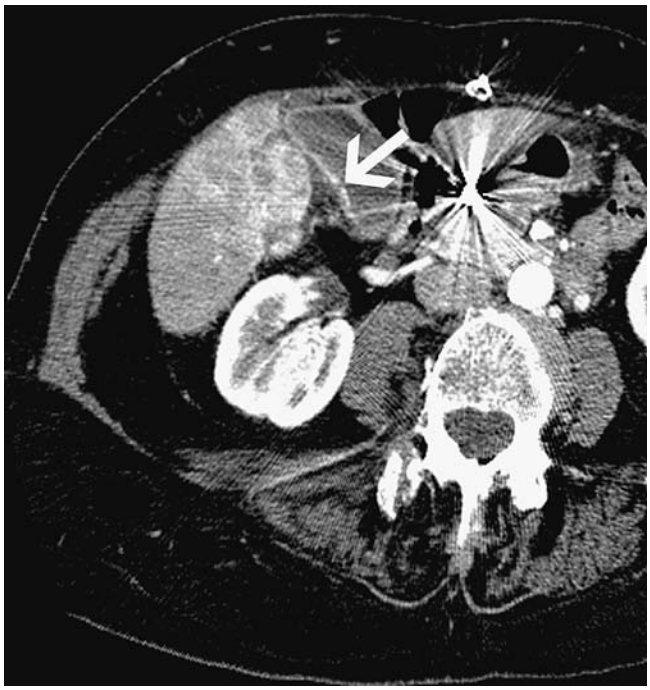

Fig. 16. Post-treatment contrast-enhanced CT demonstrates gallbladder wall enhancement with an apparent focal wall disruption (*arrow*). The patient was asymptomatic and was followed clinically.

tion-sensitivity of normal hepatic parenchyma. Radiation doses exceeding 30–35 Gy have been shown to induce hepatic dysfunction, in some cases culminating in death [50]. Although most patients recover with supportive care, few patients are refractory to medical management and succumb to their deteriorating liver function. Affected patients may present with weight gain, hepatomegaly, increased abdominal girth, anicteric ascites, and markedly elevated alkaline phosphatase weeks or months following therapy [50, 51].

Additionally, histopathologic studies may reveal a veno-occlusive pattern of liver injury characterized by central venous congestion, erythrocyte entrapment, and atrophy of hepatocytes. This clinical and pathologic spectrum is referred to as ''radiation-induced liver disease'', formerly known as ''radiation hepatitis''. This is a well known treatment-related complication seen in patients treated by external radiation sources. These signs and symptoms generally occur in the absence of cancer progression.

Although transcatheter directed internal radiation may theoretically predispose patients to similar clinical outcomes, it has only rarely been reported. In one published retrospective study of 45 consecutive patients treated with Y90 resin microspheres [52], 9 developed radioembolization-induced liver disease (REILD) characterized by jaundice and ascites within 8 weeks following treatment. All these patients developed significant hyperbilirubinemia (>3 mg/dL), elevated alkaline phosphatase (ALP), and gamma-glutamyl transpeptidase (GGTP). Rapid clinical progression was observed in 3 patients with bilirubin levels exceeding 20 mg/dL. Liver biopsies in two of these patients demonstrated veno-occlusive disease. Six of the nine patients recovered with conservative management. The authors concluded that patients with chemorefractory malignancies with pre-treatment elevated bilirubin levels were significantly more likely to develop REILD following whole liver treatments with Y90.

Young et al. examined the relationship between radiation dose and the occurrence of liver toxicities in patients who underwent two or more treatments with Y90 radioembolization [53]. Liver toxicities were reported using the National Cancer Institute Common Toxicity Criteria for

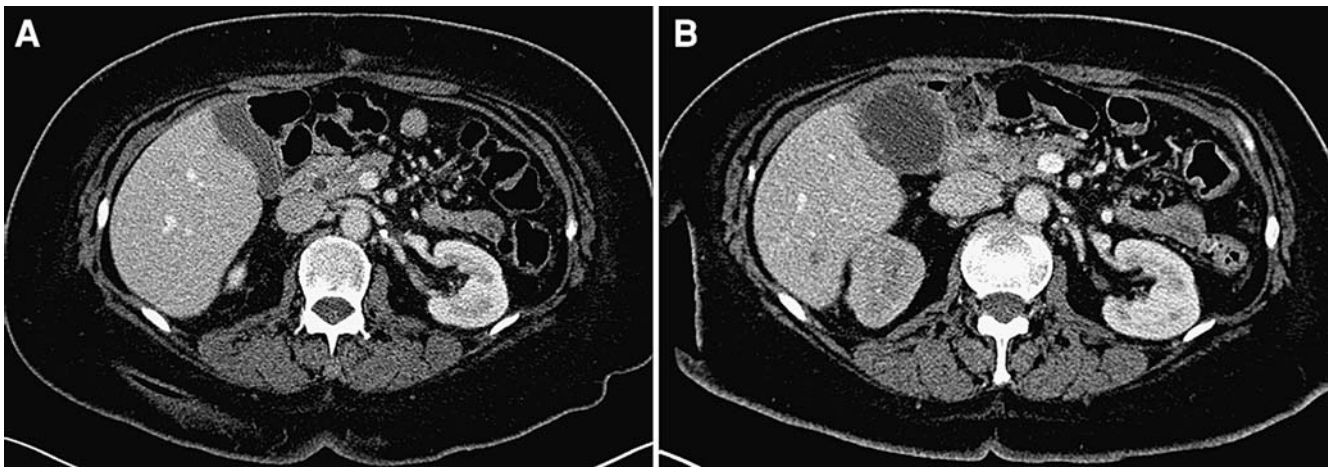

Fig. 17. (**A**) In a different patient than in Fig. 16, pre-treatment contrast-enhanced CT demonstrates a normal gallbladder. (**B**) Post-treatment contrast-enhanced CT demonstrates a small amount of pericholecystic fluid and an abnormally thickened enhancing gallbladder wall—findings indicative of cholecystitis. The patient was symptomatic with right upper quadrant pain that resolved after 2 weeks. Persistent pain that would not have resolved may have necessitated a cholecystectomy.

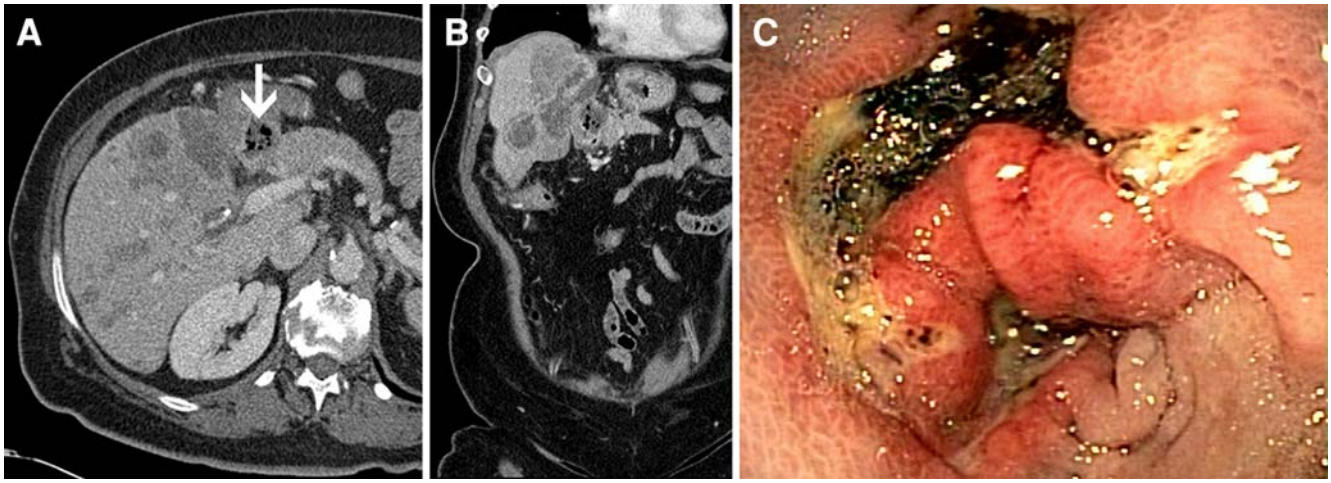

Fig. 18. (**A**) Contrast-enhanced CT scan of a patient with multifocal cholangiocarcinoma treated with Y90. The patient developed a gastroduodenal ulcer following therapy. Note air in the ulcer and a thickened pyloric wall (*arrow*). (**B**) In the same patient as (**A**), coronal contrast-enhanced CT scan demonstrates air in the ulcer and a thickened pyloric wall. (**C**) This patient had confirmed ulceration at endoscopy.

grade 3–4 elevations in ALT, AST, Albumin, ALP, and total bilirubin following therapy. The investigators showed that patients with Okuda stage I disease were able to tolerate a significantly higher number of treatments, corresponding to higher cumulative radiation doses, when compared to patients with Okuda stage II disease before the occurrence of liver toxicities. The authors concluded that, as radiation doses increases, a potential compromise in liver function may ensue.

Although radiation-induced liver disease has historically limited the use of external radiation therapy for hepatic malignancies, tumoricidal doses of radiation can be delivered to portions of the liver with virtually no adverse clinical outcomes. Selective and superselective injections have obviated this risk.

Discussion

Radiographic imaging plays a pivotal role in evaluating the effectiveness of oncologic therapeutic interventions. Assessments rely on the images obtained pre- and post-treatment and the studies are compared to determine

response. Given that both HCC and ICC are complex and heterogeneous malignancies, early follow-up or single biomarker assessments may be misleading.

Investigators have shown that the median time to partial response for patients with HCC was between 75 and 82 days following therapy [24, 25], whereas the median time to response by necrosis and combined criteria (necrosis and RECIST) was 30 and 31 days, respectively [22]. The use of a combination of biomarkers following Y90 treatment permits for a more robust assessment of tumor response.

Functional studies provide early sensitive clinical biomarkers for predicting Y90 treatment response [30]. DW-MRI has been shown to detect relatively small changes in tissue microstructure and, as a result, may differentiate viable from necrotic tissue based on these differences earlier in the post-treatment follow-up period. Given that radioembolization generally induces tumor necrosis before gross tumor volume reduction, DW-MRI should serve as an important surrogate marker for quantifying the early response to treatment.

The utility of PET for assessing HCC response to treatment remains unclear [54]. Conversely, ICCs are generally FDG avid tumors and demonstrate intense activity at PET imaging [37]. As a result, PET serves as an important adjunct for post-treatment response assessment in patients with ICCs.

Serum AFP levels are not uniformly elevated in all patients with HCC. For patients with baseline elevated pre-treatment AFP levels, tumor marker reductions following Y90 therapy may signify a positive response to treatment, even in the absence of tumor shrinkage. Unfortunately, there are no specific tumor markers for cholangiocarcinoma. Although CA 19-9, CEA, and CA 125 are the most widely used serum tumor markers, there is no evidence that measuring these markers are useful in monitoring tumor progression or response.

A potentially lethal complication characterized by signs and symptoms of liver failure has been shown to occur following external beam radiation therapies. The mechanism involves irradiating normal parenchyma beyond its tolerable limits. Although this is a theoretical concern for Y90 treated patients with primary liver malignancies, it has only been shown to occur in patients with metastatic disease who had failed on standard of care polychemotherapies [52]. Treating focal hepatic segments using selective and superselective techniques has, for the most part, obviated this risk.

Benign imaging findings commonly occur following Y90 embolotherapy. Findings such as perivascular edema, peritumoral ring enhancement, radiation effect, and increased gallbladder wall enhancement are generally not associated with clinical sequelae. Additionally, imaging features suggestive of radiation cholecystitis are often identified in asymptomatic patients. Similarly, biliary changes may occur following treatment and these findings commonly occur in the absence of clinical or biochemical alterations. Hepatic fibrosis to the treated segment or lobe is yet another benign imaging finding following therapy.

The most common complication arising from the use of Y90 radioembolization is non-target organ radiation. It is important that these iatrogenic complications be recognized early so that timely intervention is carried out. Symptomatic right upper quadrant pain, nausea, and vomiting combined with imaging findings of a thickened gallbladder and pericholecystic fluid should raise concern for radiation-induced cholecystitis. Likewise, gastrointestinal ulceration should be ruled out in patients presenting with epigastric discomfort, anorexia, and coffee-ground emesis. Other treatment-induced complications include biliary dyskinesias, bilomas, and abscesses. These are associated with considerable morbidity but are generally not-life threatening, provided that immediate interventions are instituted.

Conclusion

Ultimately, the goal of imaging following Y90 radioembolization is to serve as a successful surrogate endpoint for a patient's response to therapy. Thus, tumor shrinkage, tumor necrosis, tumor marker reduction, cellular changes indicative of non-viability at DW-MRI, and decreased FDG uptake have all been used with varying success to measure the response to treatment. For patients with HCC, tumor response following treatment has been the only predictive variable shown to correlate with survival [55]. Although a single biomarker may or may not demonstrate the Y90 response to treatment, the combination of biomarkers are likely to more accurately and reliably measure the overall therapeutic efficacy of this therapy.

References

1. Parkin DM, Bray F, Ferlay J, Pisani P (2005) Global cancer statistics, 2002. CA Cancer J Clin 55:74–108
2. El-Serag HB (2002) Hepatocellular carcinoma: an epidemiologic view. J Clin Gastroenterol 35:S72–S78
3. El-Serag HB, Rudolph KL (2007) Hepatocellular carcinoma: epidemiology and molecular carcinogenesis. Gastroenterology 132:2557–2576
4. Bruix J, Sherman M (2005) Management of hepatocellular carcinoma. Hepatology 42:1208–1236
5. Sato K, Lewandowski RJ, Bui JT, et al. (2006) Treatment of unresectable primary and metastatic liver cancer with Yttrium-90 microspheres (TheraSphere(R)): assessment of hepatic arterial embolization. Cardiovasc Intervent Radiol 29:522–529
6. Salem R, Thurston KG (2006) Radioembolization with 90Yttrium microspheres: a state-of-the-art brachytherapy treatment for primary and secondary liver malignancies: part 1: technical and methodologic considerations. J Vasc Interv Radiol 17:1251–1278
7. Salem R, Thurston KG, Carr BI, et al. (2002) Yttrium-90 microspheres: radiation therapy for unresectable liver cancer. J Vasc Interv Radiol 13:S223–S229
8. Dancey JE, Shepherd FA, Paul K, et al. (2000) Treatment of nonresectable hepatocellular carcinoma with intrahepatic 90Y-microspheres. J Nucl Med 41:1673–1681

9. Russell JL, Carden JL, Herron HL (1988) Dosimetry calculations for yttrium-90 used in the treatment of liver cancer. Endocurietherapy/Hyperthermia Oncol 4:171–186
10. Salem R, Thurston KG (2006) Radioembolization with 90Yttrium microspheres: a state-of-the-art brachytherapy treatment for primary and secondary liver malignancies: part 2: special topics. J Vasc Interv Radiol 17:1425–1439
11. Kennedy A, Nag S, Salem R, et al. (2007) Recommendations for radioembolization of hepatic malignancies using yttrium-90 microsphere brachytherapy: a consensus panel report from the radioembolization brachytherapy oncology consortium. Int J Radiat Oncol Biol Phys 68:13–23
12. Ibrahim SM, Lewandowski RJ, Sato KT, et al. (2008) Radioembolization for the treatment of unresectable hepatocellular carcinoma: a clinical review. World J Gastroenterol 14:1664–1669
13. Covey AM, Brody LA, Maluccio MA, et al. (2002) Variant hepatic arterial anatomy revisited: digital subtraction angiography performed in 600 patients. Radiology 224:542–547
14. Allen PJ, Stojadinovic A, Ben-Porat L, et al. (2002) The management of variant arterial anatomy during hepatic arterial infusion pump placement. Ann Surg Oncol 9:875–880
15. Carr BI (2002) Hepatic artery chemoembolization for advanced stage HCC: experience of 650 patients. Hepatogastroenterology 49:79–86
16. Chun HJ, Byun JY, Yoo SS, Choi BG (2003) Added benefit of thoracic aortography after transarterial embolization in patients with hemoptysis. AJR 180:1577–1581
17. Arora R, Soulen MC, Haskal ZJ (1999) Cutaneous complications of hepatic chemoembolization via extrahepatic collaterals. J Vasc Interv Radiol 10:1351–1356
18. Ueno K, Miyazono N, Inoue H, et al. (1995) Embolization of the hepatic falciform artery to prevent supraumbilical skin rash during transcatheter arterial chemoembolization for hepatocellular carcinoma. Cardiovasc Intervent Radiol 18:183–185
19. Inaba Y, Arai Y, Matsueda K, et al. (2001) Right gastric artery embolization to prevent acute gastric mucosal lesions in patients undergoing repeat hepatic arterial infusion chemotherapy. J Vasc Interv Radiol 12:957–963
20. Chung JW, Park JH, Han JK, et al. (1996) Hepatic tumors: predisposing factors for complications of transcatheter oily chemoembolization. Radiology 198:33–40
21. Therasse P, Arbuck SG, Eisenhauer EA, et al. (2000) New guidelines to evaluate the response to treatment in solid tumors. European Organization for Research and Treatment of Cancer, National Cancer Institute of the United States, National Cancer Institute of Canada. J Natl Cancer Inst 92:205–216
22. Keppke AL, Salem R, Reddy D, et al. (2007) Imaging of hepatocellular carcinoma after treatment with yttrium-90 microspheres. AJR 188:768–775
23. Atassi B, Bangash AK, Bahrani A, et al. (2008) Multimodality imaging following 90Y radioembolization: a comprehensive review and pictorial essay. Radiographics 28:81–99
24. Kulik LM, Atassi B, van Holsbeeck L, et al. (2006) Yttrium-90 microspheres (TheraSphere(R)) treatment of unresectable hepatocellular carcinoma: downstaging to resection, RFA and bridge to transplantation. J Surg Oncol 94:572–586
25. Salem R, Lewandowski RJ, Atassi B, et al. (2005) Treatment of unresectable hepatocellular carcinoma with use of 90Y microspheres (TheraSphere): safety, tumor response, and survival. J Vasc Interv Radiol 16:1627–1639
26. Sangro B, Bilbao JI, Boan J, et al. (2006) Radioembolization using 90Y-resin microspheres for patients with advanced hepatocellular carcinoma. Int J Radiat Oncol Biol Phys 66:792–800
27. Bruix J, Sherman M, Llovet JM, et al. (2001) Clinical management of hepatocellular carcinoma. Conclusions of the Barcelona-2000 EASL conference. European Association for the Study of the Liver. J Hepatol 35:421–430
28. Kulik LM, Carr BI, Mulcahy MF, et al. (2008) Safety and efficacy of 90Y radiotherapy for hepatocellular carcinoma with and without portal vein thrombosis. Hepatology 47:71–81
29. Liapi E, Geschwind JF, Vossen JA, et al. (2008) Functional MRI evaluation of tumor response in patients with neuroendocrine hepatic metastasis treated with transcatheter arterial chemoembolization. AJR 190:67–73
30. Deng J, Miller FH, Rhee TK, et al. (2006) Diffusion-weighted MR imaging for determination of hepatocellular carcinoma response to yttrium-90 radioembolization. J Vasc Interv Radiol 17:1195–1200
31. Deng J, Virmani S, Young J, et al. (2008) Diffusion-weighted PROPELLER MRI for quantitative assessment of liver tumor necrotic fraction and viable tumor volume in VX2 rabbits. J Magn Reson Imaging 27:1069–1076
32. Kamel IR, Bluemke DA, Ramsey D, et al. (2003) Role of diffusion-weighted imaging in estimating tumor necrosis after chemoembolization of hepatocellular carcinoma. AJR 181:708–710
33. Sarikaya I, Bloomston M, Povoski SP, et al. (2007) FDG-PET scan in patients with clinically and/or radiologically suspicious colorectal cancer recurrence but normal CEA. World J Surg Oncol 5:64
34. Miller FH, Keppke AL, Reddy D, et al. (2007) Response of liver metastases after treatment with yttrium-90 microspheres: role of size, necrosis, and PET. AJR 188:776–783
35. Kennedy AS, Coldwell D, Nutting C, et al. (2006) Resin 90Y-microsphere brachytherapy for unresectable colorectal liver metastases: modern USA experience. Int J Radiat Oncol Biol Phys 65:412–425
36. Sato KT, Lewandowski RJ, Mulcahy MF, et al. (2008) Unresectable chemorefractory liver metastases: radioembolization with 90Y microspheres–safety, efficacy, and survival. Radiology 247: 507–515
37. Khan SA, Davidson BR, Goldin R, et al. (2002) Guidelines for the diagnosis and treatment of cholangiocarcinoma: consensus document. Gut 51 Suppl 6:VI1–9
38. Kulik LM, Mulcahy MF, Hunter RD, et al. (2005) Use of yttrium-90 microspheres (TheraSphere) in a patient with unresectable hepatocellular carcinoma leading to liver transplantation: a case report. Liver Transpl 11:1127–1131
39. Lewandowski R, Salem R, Thurston K, et al. (2004) *Radiation segmentectomy of unresectable of liver carcinoma using selective infusion of intraarterial Yttrium-90 theraSphere*. Chicago: Radiological Society of North America
40. Rhee TK, Omary RA, Gates V, et al. (2005) The effect of catheter-directed CT angiography on Yttrium-90 radioembolization treatment of hepatocellular carcinoma. J Vasc Interv Radiol 16:1085–1091
41. Jakobs TF, Saleem S, Atassi B, et al. (2008) Fibrosis, portal hypertension, hepatic volume changes induced by intra-arterial radiotherapy with (90)Yttrium microspheres. Dig Dis Sci 53(9):2556–2563
42. Cherqui D, Palazzo L, Piedbois P, et al. (1994) Common bile duct stricture as a late complication of upper abdominal radiotherapy. J Hepatol 20:693–697
43. Nakakubo Y, Kondo S, Katoh H, et al. (2000) Biliary stricture as a possible late complication of radiation therapy. Hepatogastroenterology 47:1531–1532
44. Liu DM, Salem R, Bui JT, et al. (2005) Angiographic considerations in patients undergoing liver-directed therapy. J Vasc Interv Radiol 16:911–935
45. Sakamoto I, Iwanaga S, Nagaoki K, et al. (2003) Intrahepatic biloma formation (bile duct necrosis) after transcatheter arterial chemoembolization. AJR 181:79–87
46. Atassi B, Bangash AK, Lewandowski RJ, et al. (2008) Biliary sequelae following radioembolization with yttrium-90 microspheres. J Vasc Interv Radiol 19:691–697
47. Murthy R, Brown DB, Salem R, et al. (2007) Gastrointestinal complications associated with hepatic arterial yttrium-90 microsphere therapy. J Vasc Interv Radiol 18:553–561, quiz 62
48. Lewandowski RJ, Sato KT, Atassi B, et al. (2007) Radioembolization with (90)y microspheres: angiographic and technical considerations. Cardiovasc Intervent Radiol 30:571–592
49. Salem R, Lewandowski RJ, Sato KT, et al. (2007) Technical aspects of radioembolization with 90Y microspheres. Tech Vasc Interv Radiol 10:12–29
50. Ingold JA, Reed GB, Kaplan HS, Bagshaw MA, et al. (1965) Radiation hepatitis. Am J Roentgenol Radium Ther Nucl Med 93:200–208

51. Lawrence TS, Robertson JM, Anscher MS, et al. (1995) Hepatic toxicity resulting from cancer treatment. Int J Radiat Oncol Biol Phys 31:1237–1248
52. Sangro B, Gil-Alzugaray B, Rodriguez J, et al. (2008) Liver disease induced by radioembolization of liver tumors: description and possible risk factors. Cancer 112:1538–1546
53. Young JY, Rhee TK, Atassi B, et al. (2007) Radiation dose limits and liver toxicities resulting from multiple yttrium-90 radioembolization treatments for hepatocellular carcinoma. J Vasc Interv Radiol 18:1375–1382
54. Llovet JM, Beaugrand M (2003) Hepatocellular carcinoma: present status and future prospects. J Hepatol 38(Suppl 1):S136–S149
55. Llovet JM, Bruix J (2003) Systematic review of randomized trials for unresectable hepatocellular carcinoma: chemoembolization improves survival. Hepatology 37:429–442